

NRC DISTRIBUTION FOR PART 50 DOCKET MATERIAL
(TEMPORARY FORM)

CONTROL NO: 14394

FILE: _____

FROM: Northern States Pwr Cor ^{1/2} Minneapolis, Mn L. O. Mayer		DATE OF DOC 12-31-75	DATE REC'D 1-2-76	LTR XXX	TWX	RPT	OTHER
TO: Mr Stello		ORIG one ;signed	CC	OTHER	SENT NRC PDR <u>XX</u> SENT LOCAL PDR <u>XX</u>		
CLASS	UNCLASS XXXXX	PROP INFO	INPUT	NO CYS REC'D 1	DOCKET NO: 50-263		

DESCRIPTION:
Ltr trans the following re incident report
dtd 10-22-75.....

ACKNOWLEDGED

DO NOT REMOVE

PLANT NAME: Monticello

ENCLOSURES:
Supplemental Evaluation Rpt on Feedwater N
Nozzle Cladding Cracks.....

(40 cys encl rec'd)

FOR ACTION/INFORMATION **1-5-76 ehf**

BUTLER (L) W/ Copies	SCHWENCER (L) W/ Copies	ZIEMANN (L) W/6Copies	REGAN (E) W/ Copies	REID(L) W/ COPIES
CLARK (L) W/ Copies	STOLZ (L) W/ Copies	DICKER (E) W/ Copies	LEAR (L) W/ Copies	
PARR (L) W/ Copies	VASSALLO (L) W/ Copies	KNIGHTON (E) W/ Copies	SPIES W/ Copies	
KNIEL (L) W/ Copies	PURPLE (L) W/ Copies	YOUNGBLOOD (E) W/ Copies	LPM W/ Copies	

INTERNAL DISTRIBUTION

REG FILE NRC PDR OGC, ROOM P-506A GOSSICK/STAFF CASE	TECH REVIEW SCHROEDER MACCARY KNIGHT PAWLICKI SHAO STELLO HOUSTON NOVAK ROSS IPPOLITO TEDESCO J. COLLINS LAINAS BENAROYA VOLLMER	DENTON GRIMES GAMMILL KASTNER BALLARD SPANGLER	ENVIRO MULLER DICKER KNIGHTON YOUNGBLOOD REGAN PROJECT LDR <i>Bevan</i> HARLESS	LIC ASST R. DIGGS (L) H. GEARIN (L) E. GOULBOURNE (L) P. KREUTZER (E) J. LEE (L) M. RUSHBROOK(L) S. REED (E) M. SERVICE (L) S. SHEPPARD (L) M. SLATER (E) H. SMITH (L) S. TEETS (L) G. WILLIAMS (E) V. WILSON (L) R. INGR 'M (L) M. DUNCAN (E)	A/T IND. BRAITMAN SALTZMAN MELTZ PLANS MCDONALD CHAPMAN DUBE (Ltr) E. COUPE PETERSON HARTFIELD (2) KLECKER EISENHUT WIGGINTON K. PARRISH (L)
-----------------------------------------------------------------------------	-------------------------------------------------------------------------------------------------------------------------------------------------------------------------------	---------------------------------------------------------------	---------------------------------------------------------------------------------------------------------	------------------------------------------------------------------------------------------------------------------------------------------------------------------------------------------------------------------------------------------------------------------------------------------------	------------------------------------------------------------------------------------------------------------------------------------------------------------------------------------------------

EXTERNAL DISTRIBUTION

- 1 - LOCAL PDR *Minneapolis, Mn*
 - 1 - TIC (ABERNATHY) (1)(2)(10)
 - 1 - NSIC (EUCHANAN)
 - 1 - ASLB
 - 1 - Newton Anderson
 - 16 - ACRS HOLDING/SENT
 - 1 - NATIONAL LABS
 - 1 - W. PENNINGTON, Rm E-201 GT
 - 1 - CONSULTANTS
 - NEWMARK/BLUME/AGBABIAN
 - 1 - PDR-SAN/LA/NY
 - 1 - BROOKHAVEN NAT LAB
 - 1 - G. ULRIKSON ORNL
- TO LA DISSES w/all extras*
- MA2*

REGULATORY DOCKET FILE COPY
NSP

NORTHERN STATES POWER COMPANY

MINNEAPOLIS, MINNESOTA 55401

December 31, 1975

Mr Victor Stello, Director
Division of Operating Reactors
U S Nuclear Regulatory Commission
Washington, DC 20555

Dear Mr Stello:

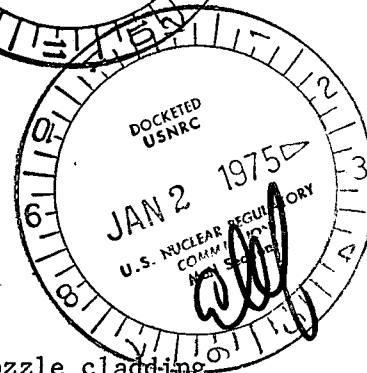
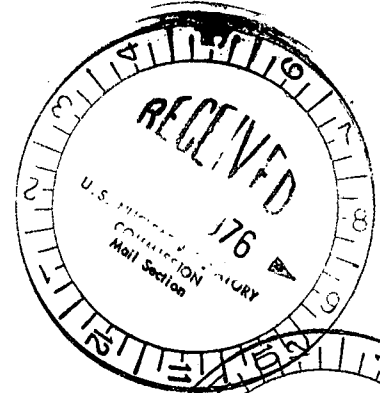
MONTICELLO NUCLEAR GENERATING PLANT
Docket No. 50-263 License No. DPR-22

Supplemental Evaluation Report on
Feedwater Nozzle Cladding Cracks

Attached is the supplemental evaluation report covering feedwater nozzle cladding crack experience at Monticello and initially reported in a Licensee Event Report dated October 22, 1975 (AO 75-20).

There are a number of additional items bearing on the conduct and quality of the grinding repairs and modified sparger replacement which should be mentioned that are not included in the attached report. The following items increase our confidence in the repair-replacement work which we believe should minimize the probability and extent of recurrence.

1. A significant effort was expended to optimize working conditions in the vessel to achieve optimum worker performance. This included the decontamination and shielding of the vessel wall; use of air handlers and vacuuming to maintain a clean working area; installation of a stable work platform; providing full supplied-air; and use of attendants to assist workers in suitup and unsuiting upon entry and exit from the in-vessel work area.
2. Level I penetrant inspection work was performed by a volunteer group of engineers and supervisors who are full time NSP employees. This approach provided a technically competent and conscientious working group who understood the significance and importance of the inspection effort in this application.
3. The penetrant inspection procedure for this application was amended to require a minimum penetrant dwell time of 15 minutes and a minimum developer dwell time of 25 minutes. We believe this amended procedure significantly improved the sensitivity of the inspection method to indicate any presence of small, tight cracks. Further, the acceptance criteria permitted no linear indication and no spot indications for final acceptance.



14394

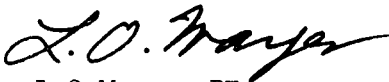
NORTHERN STATES POWER COMPANY

Mr Victor Stello
Page 2
December 31, 1975

4. As-left grinding repairs were determined by use of etching, dye-marking and replication casting techniques, thus providing accurate dimensioned definition of all repair grinding which penetrated the carbon steel material for use in the stress evaluation.
5. In addition to actual repair grinding, the outer 1/32 to 1/16 inch of clad surface materials was removed using a "flapper-wheel" as part of the surface preparation for penetrant inspections. We believe this process has removed "tired" material which may have had a larger portion of its usage factor consumed by previous service exposure, and that this significantly reduces the probability of crack indication recurrence.
6. The thermal sleeves of the replacement spargers were machined to final interference fit dimension prior to installation rather than sizing by cold-work expansion methods. We believe this increases the probable service life integrity of the fit because the sleeve starts without "memory" of cold work expansion.

In our judgment, all of the above increase our confidence that the unit was returned to service free of detectable indications in the nozzle area and that all practicable measures were taken to minimize service related recurrence of such indications.

Yours very truly,



L O Mayer, PE
Manager of Nuclear Support Services

LOM/ak

Attach

cc: J G Keppler
G Charnoff
Minnesota Pollution Control Agency
Attn: J W Ferman

NEDC-21120
SPECIAL REPORT
Class II
November 1975
75NED63

MONTICELLO
FEEDWATER NOZZLE CLADDING CRACK
REPAIR REPORT

NUCLEAR ENERGY SYSTEMS DIVISION
GENERAL ELECTRIC COMPANY
FOR
NORTHERN STATES POWER COMPANY

J. E. Charnley

Approved:



I. R. Kobsa, Manager
Operating Plants Reactor Assembly and
Performance Evaluation

Docket 50-263

BOILING WATER REACTOR SYSTEMS DEPARTMENT • GENERAL ELECTRIC COMPANY
SAN JOSE, CALIFORNIA 95125

33p/33/RA&PVD
WCC/12-75

GENERAL  ELECTRIC

TABLE OF CONTENTS

	<u>Page</u>
1.0 INTRODUCTION	1-1
2.0 SUMMARY AND CONCLUSIONS	2-1
3.0 DISCUSSION	3-1
3.1 Description of As-Found Conditions	3-1
3.2 Repair of Indications and Description of "As-Left" Conditions	3-2
3.3 Stress Evaluation on "As-Left" Conditions	3-2
3.4 Fracture Mechanics Evaluation	3-8
3.5 Fatigue Analysis-Crack Initiation and Growth	3-14
3.6 Grind-Out Weld Repair Evaluation	3-21
3.7 Corrective Actions	3-22
3.8 Corrosion Evaluation	3-23
4.0 SAFETY EVALUATION	4-1
5.0 REFERENCES	5-1

1.0 INTRODUCTION

The feedwater nozzle corner radii of the Monticello Reactor were inspected for cracks during the scheduled outage which began on September 11, 1975 (based on recent experiences at the Millstone 1, Dresden 2 and 3, Quad Cities 2, and Browns Ferry 1 plants). The dye penetrant examination of the cladding on the feedwater nozzle corner radii showed many linear indications. All four nozzles had indications. The total number of indications was approximately 180. These indications were completely removed by grinding to a maximum depth of approximately 1/2-in. from the original cladding surface. The deepest penetration into base metal was 1/4-in.

This report describes the cracking, the method of removal and final surface conditions; stress evaluation of the effects of the grindout cavities; a probable cause of cracking; a fracture mechanics evaluation of crack penetration into base metal; and the corrective actions taken.

2.0 SUMMARY AND CONCLUSIONS

Examination and analyses of the feedwater nozzles indicate that the cracking in the vessel shell to nozzle radius most probably resulted from high cycle thermal fatigue attributable to excessive bypass flow around the feedwater sparger thermal sleeves. It is believed that this bypass feedwater flow caused rapid temperature fluctuations in the affected area, a phenomena which will be reduced by the interference fit feedwater spargers which were installed after the cracks were ground out. The replacement spargers are similar to those installed in Quad Cities 2, Millstone, and Dresden 2 and 3.

A fracture mechanics analysis based upon ASME Section XI 1974 edition with addenda to and including Summer 1975 addenda was performed to determine the permissible flaw depth and in no case did the detected cracks equal or exceed the end-of-life allowable flaw. Stress evaluations indicate that these grindouts do not violate the ASME code design rules.

Periodic surveillance of the nozzle corner will be performed.

The methods employed in removing the cladding cracks and the corrective action associated with the replacement feedwater spargers to minimize the probability of a recurrence of such defects assure a safe return to full power operation for Monticello.

3.0 DISCUSSION

3.1 DESCRIPTION OF AS-FOUND CONDITIONS

3.1.1 Method of Examination

The reactor pressure vessel feedwater nozzle inner blend radius was inspected in compliance with Field Disposition Instruction 323/51847.

Following removal of the feedwater spargers, the Reactor Pressure Vessel (RPV) wall and feedwater nozzles were cleaned using a high pressure hydraulic cleaning process (hydrolaser) followed by cleaning of the feedwater nozzles using "flapper" wheels.

Dye penetrant inspection of the inner blend radius was conducted in accordance with ASME Code Section XI 1974 edition with addenda to and including Winter 1974 addenda, Paragraph IWA-2222 with the acceptance criteria as stated in ASME Code, Section III 1974 edition with addenda to and including Winter 1974 addenda, Paragraph NB-5350, but with no linear indications permitted.

During the crack repair program and for the final examination the same examination criteria and methods were employed.

3.1.2 Liquid Penetrant Test Results

The first PT revealed indications on all four nozzles with a total of 66 indications. Metal was ground away in approximately 1/16-in. increments followed by a PT. The total number of indications increased as longer indications branched. The maximum number of indications, approximately 180, were found after the fourth PT. The fourth PT corresponds to a depth of approximately 3/16-in. Fifty-three grindouts penetrated into base metal. The final PT did not reveal any indications. The maximum total depth of grindout was approximately 1/2-in. and the maximum depth of base metal removed was 1/4-in.

All but 12 of the indications were radially oriented with respect to the nozzle centerline. The 12 were circumferentially oriented and followed the overlay clad weld bead.

3.2 REPAIR OF INDICATIONS AND DESCRIPTION OF "AS-LEFT" CONDITIONS

3.2.1 Method of Repair

Hand-held grinders were used to remove metal in the localized area of the crack. Grinding was done in 1/16-in. increments in base metal, and in either 1/16-in. or 1/8-in. increments in cladding. After each increment a dye penetrant test was performed to determine whether the crack had been removed, and the location of remaining indications. Grindouts that were suspected of penetrating into base metal were acid-etched using Nital after crack removal.

After the indications were removed the bottom of the cavity was ground to a radius of twice the total depth of the cavity, and the sides of the grind cavities were ground to blend smoothly with the surrounding cladding metal surface with a minimum slope of 4 to 1 in base metal 2 to 1 in the cladding. A PT was performed on the blended cavity and final determination of clad base metal interface was made using demineralized water.

3.2.2 Description of "As-Left" Conditions

All base metal ground areas were measured and mapped as shown in Figures 1 through 4.

3.3 STRESS EVALUATION ON "AS-LEFT" CONDITIONS

The Reactor Pressure Vessel Stress Report contains an evaluation of the feed-water nozzle minimum design dimensions at the nozzle-to-shell junction, performed in accordance with ASME Code Section III 1965 edition including Summer 1966 edition, Paragraph N-450. It is assumed therein that 1/16-in. depth of the unclad base metal surfaces is nonexistent, as corrosion allowance. The calculation shows the required nozzle reinforcement area to be 28.30 in.², compared to available reinforcement area of 31.20 in.². The stress report

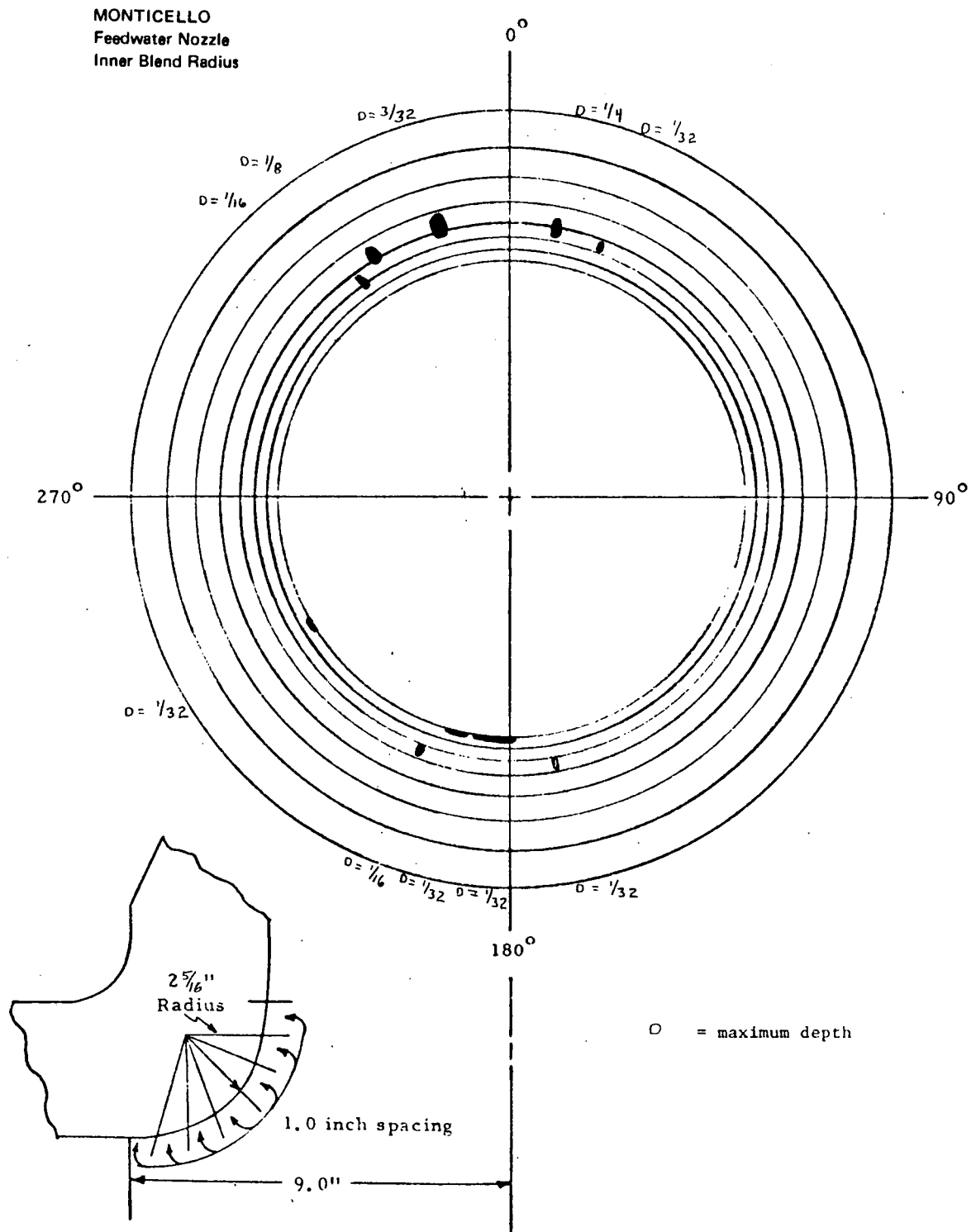


Figure 1. 45° Nozzle Base Metal Grindouts

MONTICELLO
Feedwater Nozzle
Inner Blend Radius

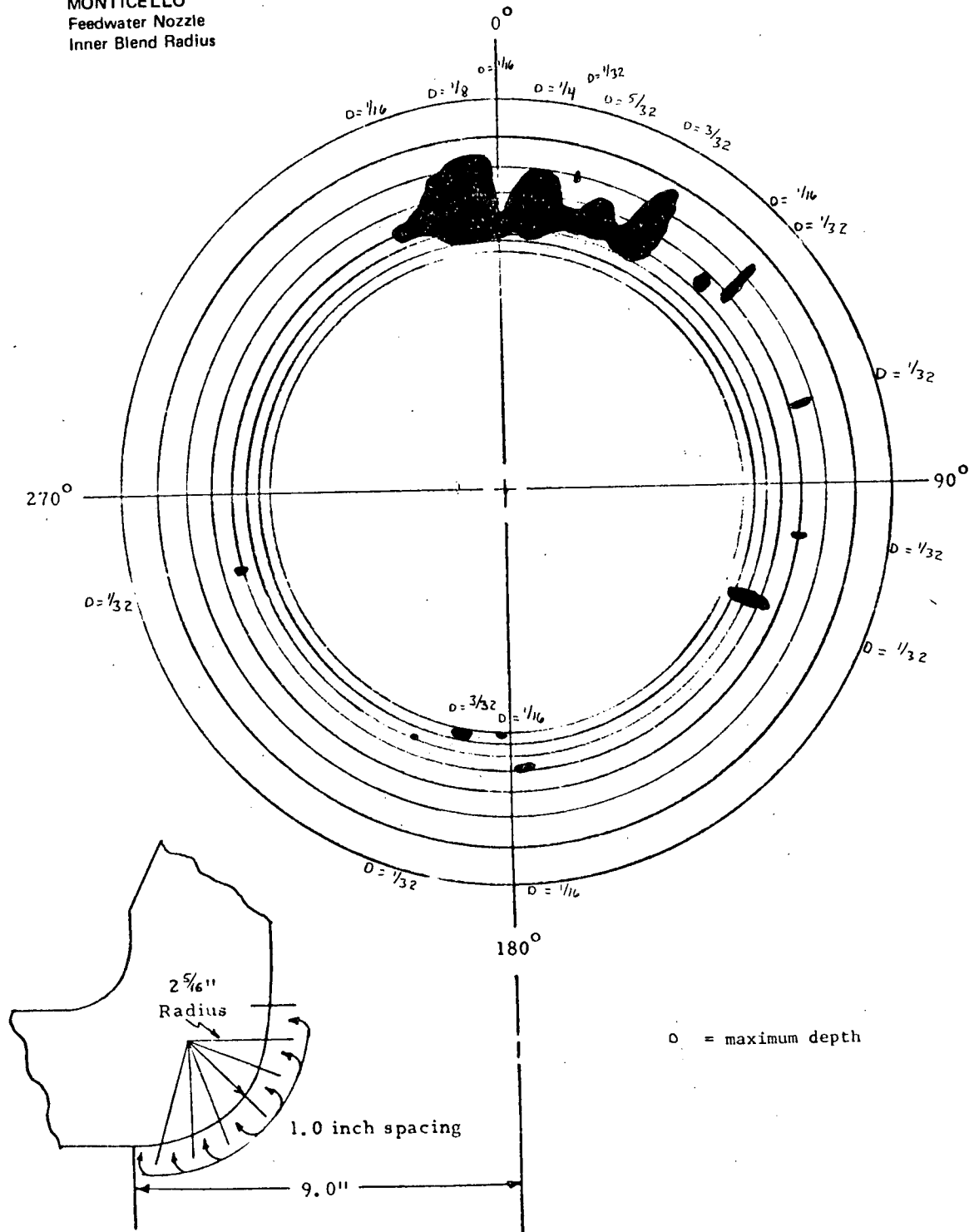


Figure 3. 225° Nozzle Base Metal Grindouts

MONTICELLO
Feedwater Nozzle
Inner Blend Radius

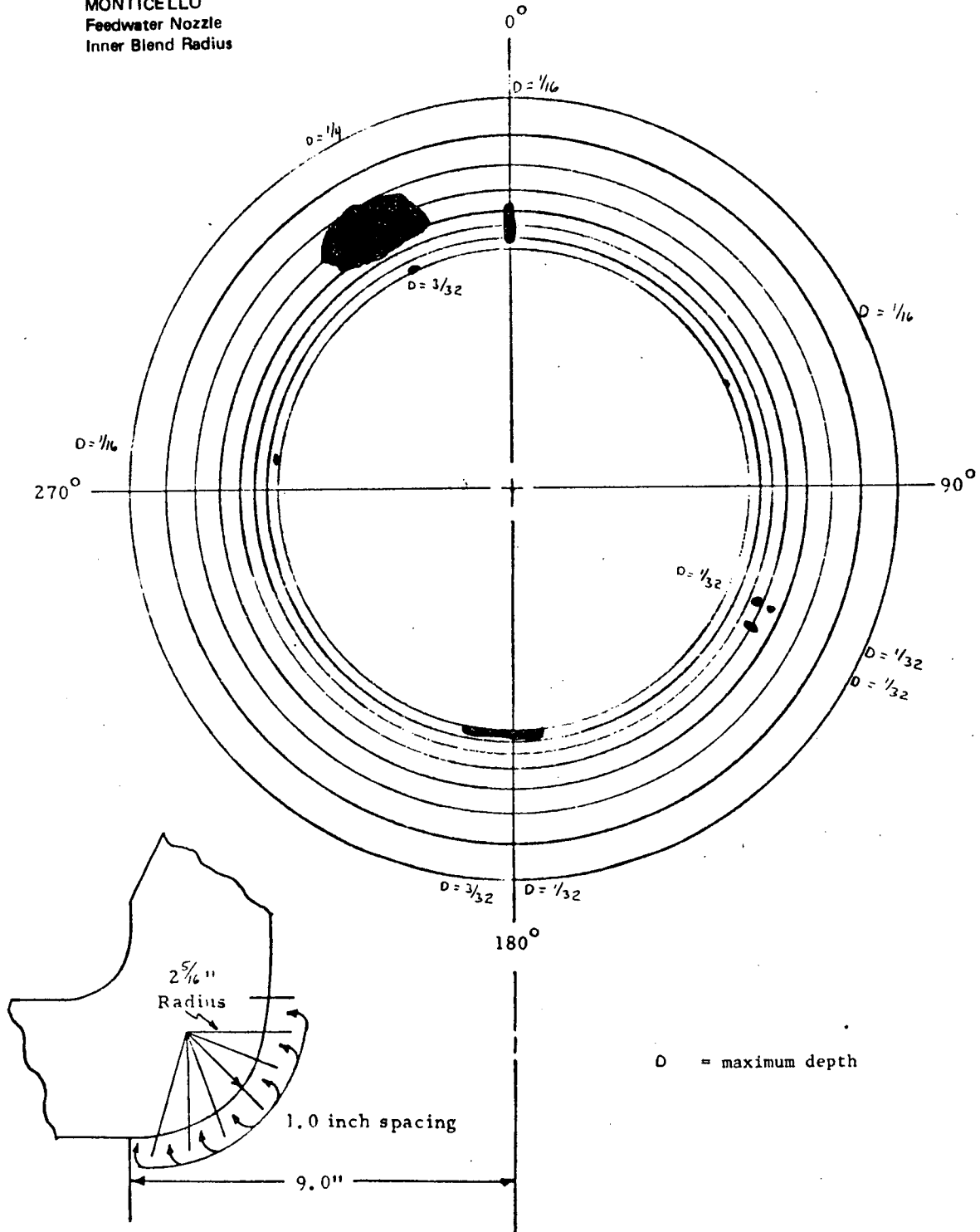


Figure 4. 315° Nozzle Base Metal Grindouts

does not account for all the available reinforcement area. An additional 2.2 in.² is available. One-half of the reinforcement area must be on each side of the nozzle centerline.

Removal of base metal from the nozzle corner increases the required reinforcement area by the amount of low-alloy base material removed, measured as the largest cross-section area of removed metal lying in a plane through the nozzle centerline. Additionally, as the low-alloy steel is no longer clad at this location, 1/16-in. depth more than was actually removed is assumed non-existent for corrosion allowance, as above. All 53 grindouts that penetrated into base metal were mapped. The nozzle corner radius location with the largest base material removal is shown in Figure 5. As indicated, the additional required reinforcement area is approximately 0.64 in.². Since the available excess reinforcement area is $(31.20 - 28.30) = 2.90\text{-in.}^2$, the additional reinforcement area required as a result of this repair is approximately 22% of that which could be removed without violation of the original code calculation and $0.64/2.9 + 2.2 = 13\%$ of actual.

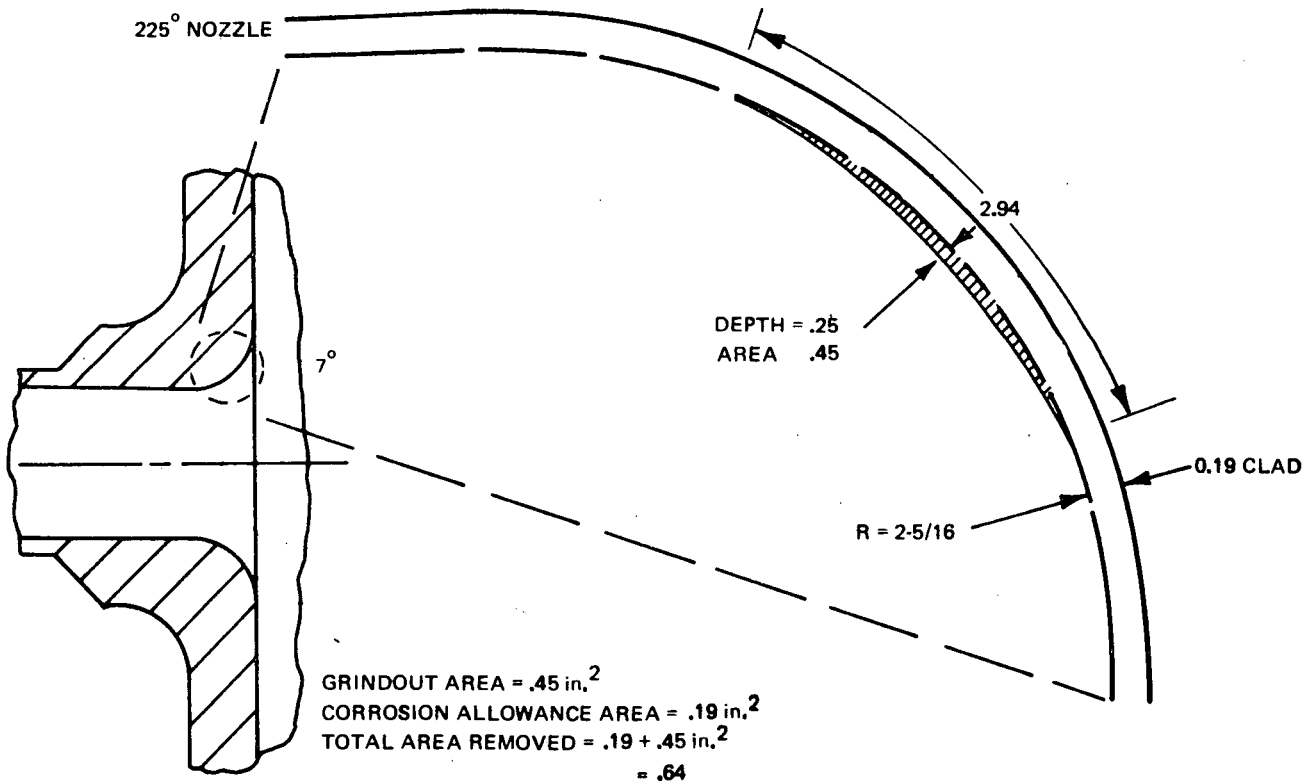


Figure 5. Largest Base Material Removal

3.4 FRACTURE MECHANICS EVALUATION

All indications have been removed by grinding and the grindouts have been blended to the outside surface using a minimum of 2:1 taper. The root of the grind cavity has been blended to provide a smooth radius with no sharp breaks in contour. Penetration into the base material occurred at some locations and the maximum depth of penetration into the base metal was 1/4-in.

The allowable flaw depth for indications in cladding surfaces for inservice examinations is 1/8-in. as prescribed in IWB-3517, Section XI 1974 edition with addenda to and including Summer 1975 addenda, ASME Code. For cracks which extend through the cladding into the base material, a fracture mechanics evaluation is also necessary if the crack is deeper than allowed by IWB-3512.

The applied stress intensity factor is due to a combination of the pressure hoop stress and the thermal stress. The stress intensity factor due to pressure alone is given by³

$$K_p = F(a,r) \sigma_h \sqrt{\pi a}$$

where

K_p = stress intensity factor due to pressure,

σ_h = hoop stress in the vessel,

a = flaw depth measured from the nozzle corner,

$F(a,r)$ = geometrical factor given in WRC-175 (Reference 3).

$$\sigma_h = \frac{PD}{2t} = \frac{1.000 \times 206}{2 \times 5.0625} = 20.4 \text{ ksi}$$

The stress intensity factor K_p due to pressure is plotted in Figure 6.

Consider the contribution from thermal stress to the applied stress intensity factor.

In a thermal analysis performed for (Reference 2) the Millstone feedwater nozzle, the maximum thermal stress at the nozzle corner was calculated to be 44 ksi for a step change in feedwater temperature from 546°F to 100°F. Since this analysis

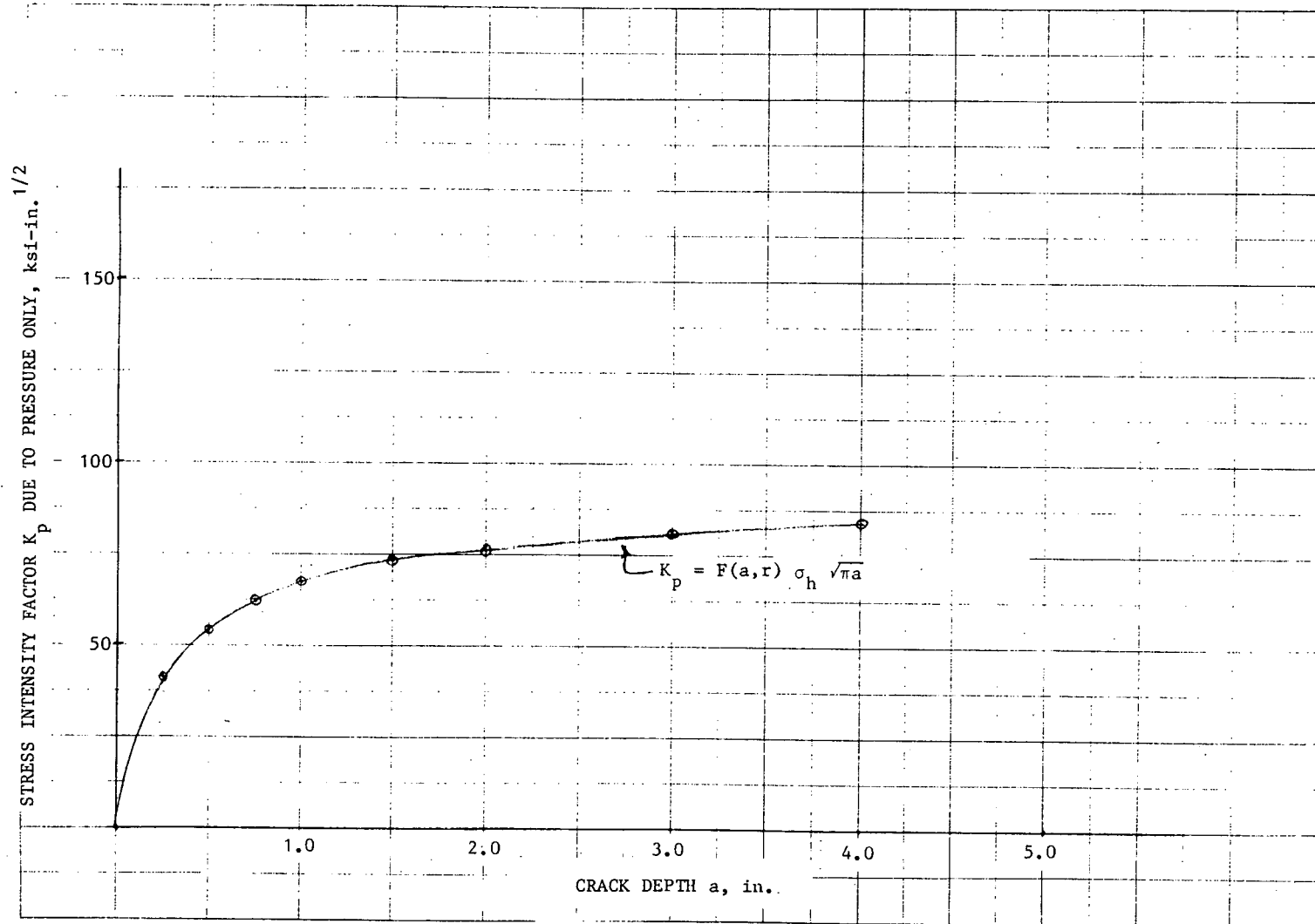


Figure 6. Pressure Stress Intensity Factor

did not take the presence of the thermal sleeve into consideration, the calculated thermal stress is conservative. The same calculated thermal stress of 44 ksi is conservatively assumed for the present analysis also.

The procedure for calculating the stress intensity factor due to the thermal stresses is not clearly defined in the literature. Two different methods will be used to characterize the thermal stress intensity factor.

3.4.1 Uniform Thermal Stress Method

This method assumes the surface thermal stress σ_{th} to be uniformly distributed through the entire thickness. This is very conservative and provides an upper bound on the applied stress intensity factor K_{th} . This is given by

$$K_{th} = 1.1 \sigma_{th} \sqrt{\pi a} = 1.1 \times 44 \sqrt{\pi a}$$

where the stress intensity formulation for a surface flaw under uniform stress is used.

3.4.2 Equivalent Hoop Stress Method

In this method the effect of the thermal stress is considered by calculating an equivalent hoop stress and using the stress intensity formulation for a nozzle under pressure loading. The equivalent hoop stress is obtained by dividing the nozzle surface thermal stress σ_{th} by the stress index which is conservatively assumed to be 2.5 (Reference 3).

$$\sigma_{eq} = \sigma_{th} / 2.5 = \frac{44}{2.5} = 17.6 \text{ ksi}$$

The thermal stress intensity factor is then

$$K_{th} = F(a,r) \sigma_{eq} \sqrt{\pi a}$$

By calculating the equivalent hoop stress we are assuming that the thermal stress distribution is similar to that caused by the stress concentration due to pres-

sure loading. This is a more reasonable assumption than considering the thermal stress constant. A detailed stress analysis is expected to indicate that thermal stress decreases more rapidly than pressure stress, but models are not available to determine the distribution.

The total applied stress intensity factor K is obtained by adding the contributions due to the pressure stresses and the thermal stresses.

Figure 7 shows the total applied stress intensity factor calculated by the two different techniques. The thermal analysis performed in Reference 2 as well as the actual temperature measurements have shown that the nozzle corner is at a temperature high enough to retain a toughness level of 200 ksi-in.^{1/2}.

The critical flaw size a_c is then at the intersection of the 200 ksi-in.^{1/2} line with the applied stress intensity curve.

According to the first method where the thermal stress is assumed to be uniform, the critical flaw size is 2.05 in. It must be remembered that this calculation is based on extremely conservative assumptions that thermal stress is distributed uniformly with flaw depth. Even the calculation of the thermal stress value is conservative since the beneficial effect of the thermal sleeve is not included.

Figure 7 also shows that for the second method based on the equivalent hoop stress technique the critical flaw does not occur (i.e., the crack would penetrate the wall and leak without growing unstably).

The fact that a nozzle corner flaw would "leak before break" is supported by the results of the HSST program. For example, in the test on vessel 5 at 190°F with a nozzle corner flaw of 1.2 in., failure occurred at 2.75 times the ASME design pressure and the mode of failure was leakage. The "leak before break" feature provides additional assurance of safety.

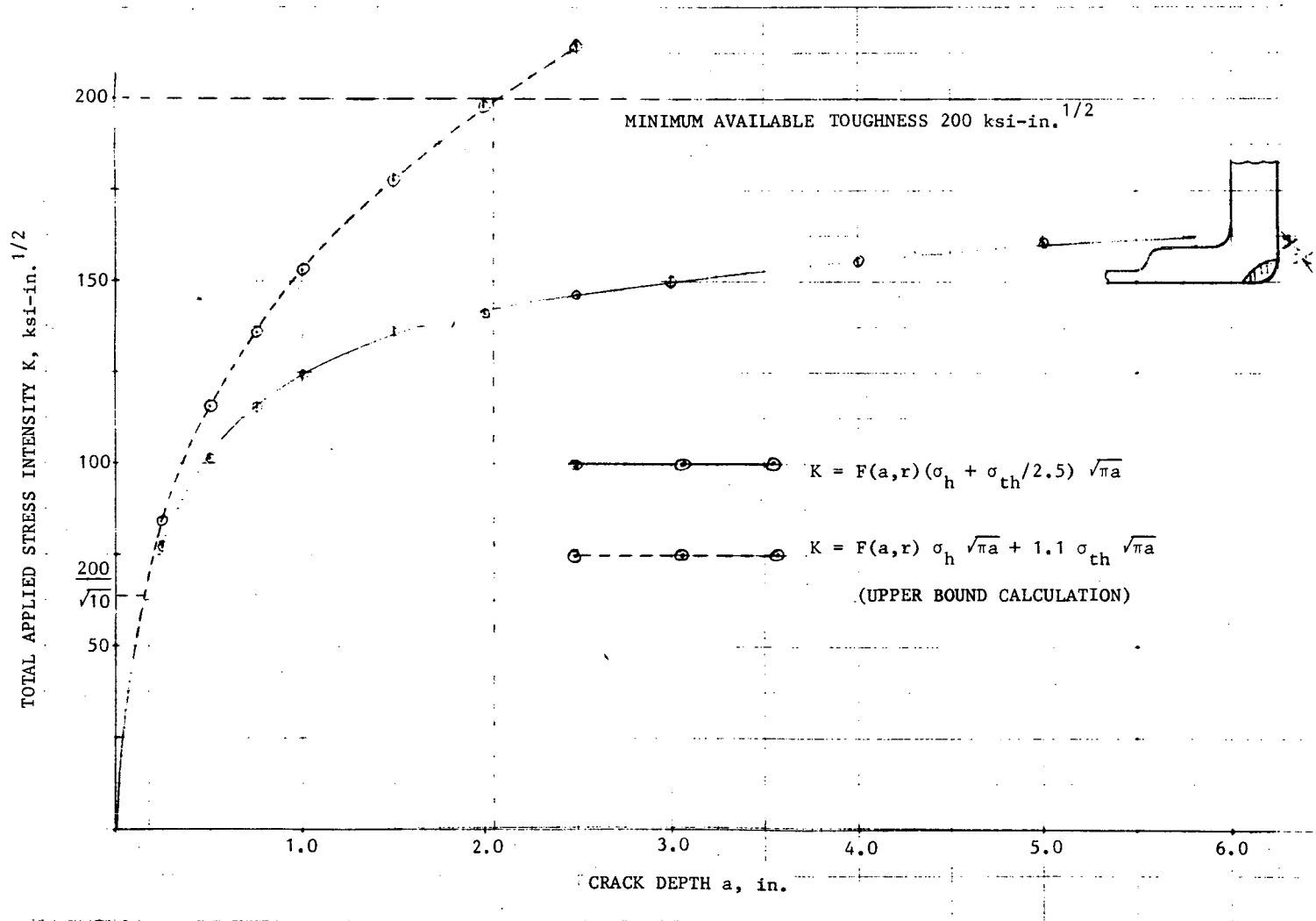


Figure 7. Total Stress Intensity Factor

It can therefore be concluded that the critical flaw size is not less than 2 in. and is probably closer to 8 in. The exact value can be determined only by detailed stress analysis.

According to Section XI ASME Code the allowable end-of-life flaw size can be obtained by dividing the critical flaw size by a factor of 10 or alternately by calculating the critical size for the case where the toughness is taken to be $\frac{1}{\sqrt{10}}$ times the actual available fracture toughness. Because of the non-linear dependence of the stress intensity on the local stress these two approaches are not equivalent for the nozzle corner crack problem. Depending on the method used the allowable end-of-life flaw size ranges from 0.17 in. to at least 0.8 in. ($\frac{1}{10}$ the wall thickness) as shown on Figure 7. The equivalent hoop stress method is the more realistic method and therefore based on a conservative interpretation of Section XI the allowable end-of-life flaw size is 0.8. Thus all observed cracks were less than the end-of-life allowable.

Since the critical flaw size is greater than the wall thickness, a flaw cannot grow to the critical size. Thus the end-of-life allowable flaw size cannot, strictly speaking, be determined and the criteria are not applicable.

3.5 FATIGUE ANALYSIS-CRACK INITIATION AND GROWTH

Temperature fluctuations with ranges up to 125°F and frequency of up to 1 Hz, have been observed in the vicinity of the blend radius of the feedwater nozzle in tests run under normal reactor operation at Millstone with feedwater spargers similar to those replaced at Monticello.¹ This design used a slipfit between the thermal sleeve and the nozzle which permitted bypass leakage past the thermal sleeve. It is believed that the thermal cycling observed at Millstone resulted in part from the bypass leakage flow into the nozzle. Cracks were discovered in the Millstone feedwater nozzle cladding near the points where significant thermal cycling was observed. Analysis also showed that these cracks could have been initiated by thermal fatigue resulting from the observed temperature cycling.

Although temperature measurements have not been made at Monticello, it is believed that Monticello has also experienced thermal cycling comparable to that observed at Millstone because of the similar slipfit sparger design used at Monticello. Heat transfer calculations based on the original Monticello geometry have been performed. These calculations considered a range (0.008 to 0.030 inch) of radial gap between the leakage land and the thermal sleeve. At rated conditions the temperature of the leakage water in the vicinity of the blend radius was calculated to be 130°F to 150°F colder than reactor water. Thus fluid temperature cycling of this magnitude is predicted, which corresponds to blend radius temperature cycling of approximately 90°F to 130°F. This result supports the conclusion that leakage flow is the cause of the observed thermal cycling.

Figure 8, which is based on ASME Section III fatigue curve extrapolated to 10¹⁰ cycles and on temperature fluctuations of 1 Hz, shows that 125°F cycling at rated conditions would begin initiating cracks between 300 and 45,000 hours. It is expected that some cracks would initiate in less than one year of rated operation. Thermal cycling during startup and other conditions can be significantly higher than 125°F thus decreasing the time required to initiate cracks.

Based on the frequency and amplitude of the thermal cycling it is concluded that the high cycle thermal stresses would drive the cracks to a depth of approximately 0.1 inch. Further growth must be attributed to another cause.

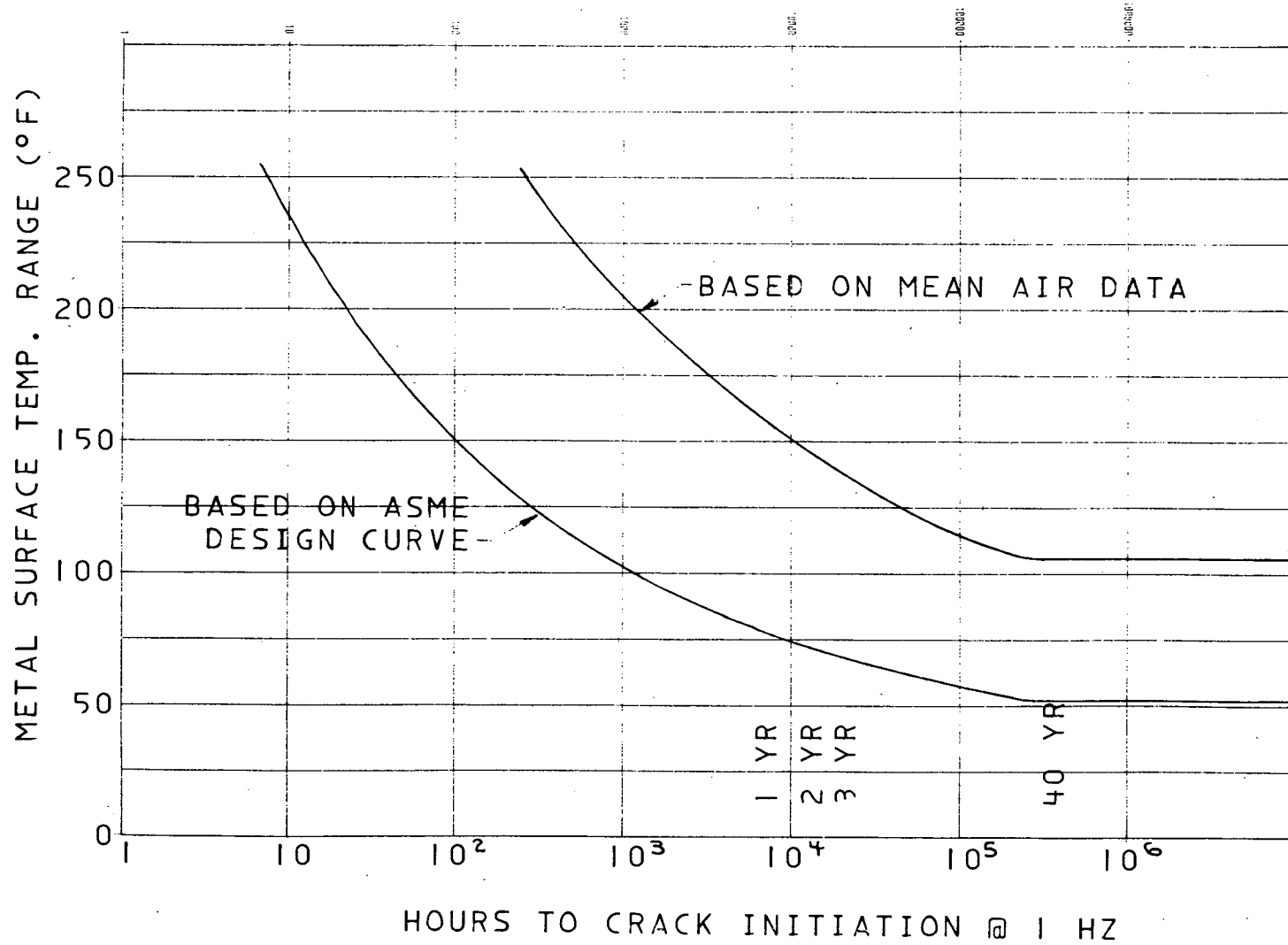


Figure 8. Fatigue Crack Initiation

Metallurgical examination of the material near the cracks at Millstone also supports the conclusion that the cracks resulted from fatigue cycling.

The second mechanism is large thermal and pressure stress cycling due to reactor startup. Crack growth in the blend radius cladding has been calculated using: (based on Reference 6)

$$a_f = \left[(a_i)^{-0.5} - (0.5) (1.4 \times 10^{-9}) N (2.5 \sqrt{\pi\sigma})^3 \right]^{-2}$$

where:

- a_f = final crack size
- a_i = initial crack size
- N = number of stress cycles
- σ = stress range using the equivalent hoop stress method

$$= \frac{\sigma_{th}}{2.5} + \sigma_h \quad (\text{pressure plus thermal cycle})$$

or

$$= \frac{\sigma_{th}}{2.5} \quad (\text{thermal cycle})$$

Crack growth in the base metal at the blend radius has been calculated using: (ASME Section XI, Appendix A)

$$a_f = \left\{ (a_i)^{-0.863} - (0.863) (0.3795 \times 10^{-9}) N [F(a,r) \sqrt{\pi\sigma}]^{3.726} \right\}^{-1.159}$$

Crack growth is plotted on Figure 9 using the values in Table 1. Each startup cycle consists of one cycle of pressure plus thermal, and five thermal cycles. The data points do not all lie on a smooth curve as the geometrical factor was changed in a stepwise manner. Figure 9 shows that a 0.1-inch crack will grow to a 0.44-inch crack in 78 cycles and to a 0.50-inch crack in 88 cycles.

Thus the existence of cracks up to a total depth of 0.5 inch is attributed to initiation by high cycle fatigue and growth by pressure plus thermal cycling.

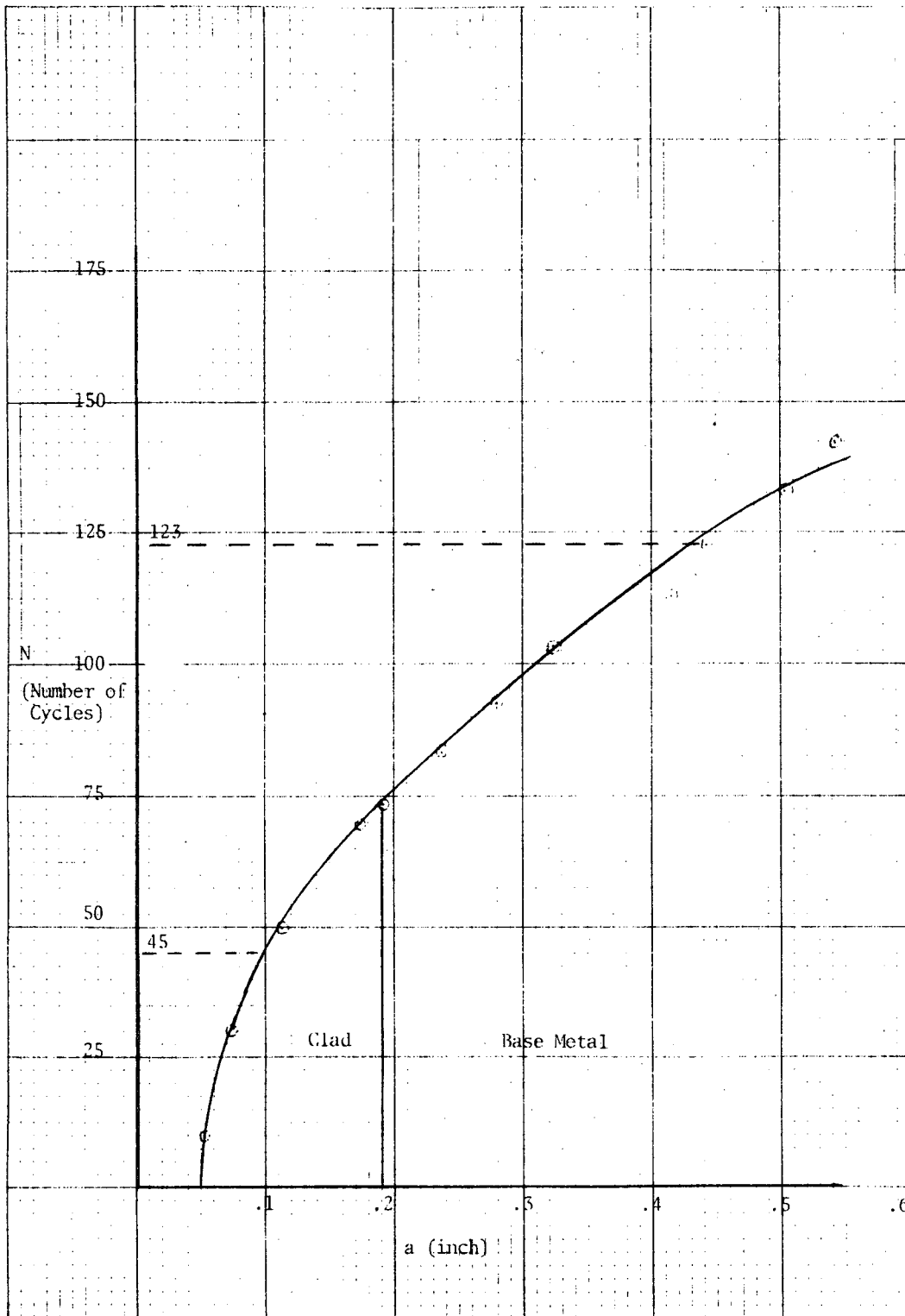


Figure 9. Crack Growth

Table 1
CRACK GROWTH

CLADDING

a_i (in.)	a_f (in.)	N (cycles)	σ_{th} (ksi)	σ_h (ksi)
0.05-in.	0.057	10	96	20.4
	0.078	30	96	20.4
	0.112	50	96	20.4
	0.174	70	96	20.4
	0.183	72	96	20.4

BASE METAL

a_i (in.)	a_f (in.)	N (cycles)	σ_{th} (ksi)	σ_h (ksi)	F(a, r)
0.19	0.0	73	44	20.4	NA
	0.238	83	44	20.4	2.4
	0.282	93	44	20.4	2.3
	0.324	103	44	20.4	2.2
	0.416	113	44	20.4	2.2
	0.441	123	44	20.4	2.1
	0.501	133	44	20.4	2.05
	0.555	143	44	20.4	2.00

The as-left condition has been evaluated for fatigue life. Two conditions were considered: the bottom of a grindout, and the surface of the cladding.

At the bottom of a base metal grindout:

$$\sigma_{alt} = \frac{k \sigma_h + \sigma_{th}}{2}$$

where:

$$\begin{aligned} \sigma_{alt} &= \text{alternating stress} \\ k_{max} &= 5.0 \\ \sigma_h &= 20.4 \text{ ksi} \\ \sigma_{th} &= 44.0 \text{ ksi} \\ \sigma_{alt} &= 73 \text{ ksi} \\ N_{allow} &= 1450 \text{ cycles} \end{aligned}$$

The required number of remaining cycles is taken to be 90% of the total number of Monticello design cycles, which is equal to

$$(0.9) (1500) = 1350 \text{ cycles}$$

Thus the usage factor is

$$UF = \frac{1350}{1450} = 0.93$$

Therefore new cracks are not expected to initiate at the bottom of a base metal grindout if the as-left usage factor is less than 0.07 and thermal cycling of the base metal at rated conditions is less than 45°F, which corresponds to the endurance limit.

On the surface of the cladding:

$$\sigma_{alt} = \frac{k \sigma_h + \sigma_{th}}{2}$$

$$\begin{aligned}
 k &= 3.1 \text{ (stress index)} \\
 \sigma_h &= 20.4 \text{ ksi} \\
 \sigma_{th} &= 96.0 \text{ ksi} \\
 \sigma_{alt} &= 79.6 \text{ ksi} \\
 N_{allow} &= 2800 \text{ cycles}
 \end{aligned}$$

$$UF = \frac{1350}{2800} = 0.48$$

Therefore new cracks are not expected to initiate in the cladding if the as-left usage factor is less than 0.52 and thermal cycling of the cladding at rated conditions is less than 50°F which corresponds to the endurance limit.

Since the pressure stress at the blend radius is predominantly in the hoop direction, the cracks are expected to be oriented radially with respect to the nozzle and this is confirmed by the crack observation at Monticello.

The circumferential cracking inside the nozzle bore is attributed to thermal cycling coupled with lack of fusion in the original cladding.

The analysis presented here illustrates the importance of restricting the local surface temperature fluctuations in order to prevent further crack initiation. With the use of the interference fit feedwater sparger design, it is believed that the fluid temperature fluctuations will be reduced to acceptable levels. As discussed in Subsection 3.7, operating data from Millstone 1, which uses an interference fit sparger design similar to that just installed at Monticello, showed that the fluid temperature fluctuation range was within 50°F, thus confirming the effectiveness of the new design. It is therefore reasonable to conclude that thermal cycling problems are less likely to occur at Monticello with the new design spargers.

Even with minimal thermal cycling it is possible that additional cracks will initiate as the remaining material has experienced an unknown amount of fatigue damage.

3.6 GRIND-OUT WELD REPAIR EVALUATION

Based on an evaluation of the completed nozzle grindouts and available weld repair methods, it was concluded that weld repair of the areas excavated to remove cracks is not justified.

For this application, two types of weld repair after final post-weld heat treatment are possible under Section XI rules. Procedure No. 5 in IWB-4430 allows recladding those areas where the low-alloy base metal has been exposed. Therefore, this repair would be justified only if required for corrosion resistance. This is shown not to be the case in the examination of base metal corrosion characteristics given in Subsection 3.8. It is additionally shown in Subsection 3.3 that 1/16-in. depth of the exposed base metal is considered as corrosion allowance.

Procedure No. 4 in IWB-4420 could also be used prior to the above recladding to first restore the removed portions of the base metal. This would be necessary if the structural adequacy of an excavated area were insufficient. However, it is shown in Subsection 3.3 that the excavated areas satisfy the applicable Section III Code design limits, and that the amount of material removed was relatively minor.

Consideration was also given to the effects of performing weld repairs discussed above. Use of the temper-bead methods of Section XI is generally felt to involve substantial difficulty, and uncertainty.

As this type of process is infrequently applied, its qualification for this application would be partly developmental. The significant amount of structural

restraint of the repair weld areas from the adjacent vessel wall would require careful study to avoid cracking. Substantial thermal and stress analysis effort and testing would also be needed to develop the techniques for the required pre-heat, interpass, and the 450 to 550°F thermal treatments to avoid harmful gradients and distortion. Because of the restraint and heat sink effects caused by the vessel wall, the requirements for heating, cooling, and location of insulation are likely to be complex.

In summary, it is believed that weld repair of the grind-outs need not be performed, and that consideration of the design adequacy does not warrant such a repair in this case.

3.7 CORRECTIVE ACTIONS

The methods utilized to locate and remove all detected cracks assure that local discontinuities, capable of propagation, do not exist at this time.

As discussed in Subsections 3.4 and 3.5 of this report, it is important that the local surface temperature fluctuations, such as were likely to have been experienced during operation with the original spargers be reduced. The replacement feedwater spargers have been installed with an interference fit based upon measurements of the diameter of the thermal sleeves and the nozzle bores. This procedure should assure continuous contact around the circumference of the thermal sleeve, except during intermittent periods of very low feedwater temperature experienced during startup.

As a result of these design improvements, the leakage through the gap is expected to be small during full power operation. The anticipated leakage at low power levels is not expected to cause significant annular fluid temperature fluctuations in the thicker regions of the nozzles, because the small amount of leakage flow will be mixed with hot reactor water in the annulus. The effectiveness of the above design improvements has been confirmed for the similar sparger to nozzle fit-up used in the Millstone 1 sparger replacement. Operating data showed the fluid temperature fluctuations in the nozzle annulus were reduced to a maximum of 50°F for any operating condition. The effectiveness of the interference fit design will continue to be evaluated as part of the ongoing sparger design evolution.

Even with minimal thermal cycling it is possible that additional cracks will initiate, as the remaining material has experienced an unknown amount of fatigue damage. Thus it will be necessary to periodically inspect the nozzle blend radii. This inspection program will ensure that all flaws will be found substantially before they reach the critical size as determined by the most conservative calculations and before they reach the Section XI allowable size as determined by more realistic calculations.

3.8 CORROSION EVALUATION

3.8.1 General Corrosion in a BWR

General corrosion rates for carbon steel and low alloy steels have been determined in tests performed by General Electric Company. No differences in corrosion rates were noted between the carbon steels and low alloy steels. The highest corrosion rates occur in low temperature, air-saturated water which would be present prior to reactor startup, and during refueling outages. At temperatures up to 100°F, the corrosion rate of bare steel in stagnant, air-saturated water is 0.0015 in. per year. Very little corrosion occurs in the high temperature BWR water or steam. A thin, black oxide film forms very rapidly at elevated temperatures and it is protective against corrosion. The measured corrosion rates in 546°F BWR water or steam are less than 10 mgldm²/month (a corrosion rate of 17 mgldm²/month equals 0.0001 inches per year). A very conservative rate of 0.0001 in. per year for corrosion estimates on carbon steel components is assumed.

The worst case for the total corrosion of RPV nozzles would be if all low temperature corrosion occurred on bare, un-oxidized steel surfaces. The estimated corrosion on unclad nozzles would be as follows:

Assume 90% high temperature reactor operation, then
 36 years X 0.0001 in./yr = 0.0036 in.

Assume 10% low temperature exposure at 100°F for startup
 and refueling outages, then
 4 years X 0.0015 in./yr = 0.0060 in.

Total 40-year corrosion = 0.0096 in.

Actually, the high temperature oxide formed during reactor operation continues to provide corrosion protection when the reactor is shut down for refueling. Therefore, the total corrosion should be less than 0.0096 in. for a 40-year reactor lifetime.

3.8.2 Galvanic Corrosion in BWR Environment

Numerous studies^{4,5} have been made to determine whether galvanic (electro-chemical) corrosion would be a problem in nuclear reactor systems where dissimilar metals are in contact. One of the common dissimilar metal combinations found in Boiling Water Reactors consists of austenitic stainless steel joined to carbon (including low alloy) steel.

Corrosion tests performed in high-purity reactor water have shown no detrimental galvanic corrosion effects on austenitic stainless steel-carbon steel weldments or joints. Neither the general corrosion rates, nor localized corrosion of the carbon steel have been affected. Investigators attribute this lack of any galvanic corrosion to the fact that high purity BWR water has very low electrical conductivity. The conductivity is too low to promote galvanic or electro-chemical effects.

The performance of stainless steel-carbon steel couples in an operating reactor has been reported by the Argonne EBWR. This boiling water reactor employed stitch welded stainless steel cladding in the reactor pressure vessel. Cracking occurred in the sheet steel cladding which exposed the bare reactor vessel steel to the water environment. Examinations performed after several years of operation showed no evidence of detrimental general corrosion or galvanic corrosion.

4.0 SAFETY EVALUATION

The corrective actions taken, as described in Subsection 3.7 of this document, will ensure that the original design requirements of the vessel are met during future operation of the reactor. The removal of all cracks provides assurance that further propagation will not continue in these affected areas. Replacement of the feedwater spargers with improved thermal sleeve/nozzle interface will reduce the local surface temperature fluctuations to a negligible level. With respect to ASME Section XI, the governing code for inservice nuclear components, the structural integrity of the reactor pressure vessel has not been compromised, since all cracks have been completely removed. With respect to ASME Section III, the original construction code for the reactor pressure vessel, the amount of base metal removed and consequently the additional nozzle reinforcement area required are adequately compensated for by the existing available reinforcing area which remains in excess of that required by the Code. As such, a degradation of the original design requirements with regard to the low-alloy steel base metal has not occurred. Therefore, based on 10CFR 50.59, the cracks during this outage do not constitute an unreviewed safety question.

Installation of the new design feedwater spargers is expected to reduce the previously experienced local temperature fluctuations to acceptable levels thereby reducing the potential for additional cladding crack initiation. The new design feedwater spargers will also reduce the steady-state thermal stresses in the nozzle to vessel shell region because of the reduction in flow between the nozzle and the thermal sleeve.

Therefore, based on 10CFR 50.59, operation of the reactor with the new design feedwater sparger does not constitute an unreviewed safety question.

5.0 REFERENCES

1. Millstone Nuclear Power Station Unit 1, Feedwater Sparger Failure, Evaluation of Design No. 3 Test Results, Interim Report, Addendum 2, September 21, 1973.
2. "Chloride Intrusion Incident," Special Report, Millstone Nuclear Power Station Unit 1, December, 1972.
3. "PVRC Recommendation on Toughness Requirements for Ferritic Materials," WRC Bulletin 175.
4. "Technology of Steel Pressure Vessels for Water Cooled Nuclear Reactors," Edited by G. D. Whitman, et al, ORNL-NSIC-21, UC-80, December 1967.
5. Vreeland, D.C., Gaul, G.G., Pearl, W.L.," Corrosion, 17, No. 6, 269t-276t, 1961, June.
6. NEDO-20926, Evaluation of the Structural Significance of Flaws in Nuclear Piping Welds, to be issued.